Clays and Clay Minerals, Vol. 46, No. 5, 528–536, 1998.

USE AND LIMITATIONS OF SECOND-DERIVATIVE DIFFUSE REFLECTANCE SPECTROSCOPY IN THE VISIBLE TO NEAR-INFRARED RANGE TO IDENTIFY AND QUANTIFY Fe OXIDE MINERALS IN SOILS

A. C. SCHEINOST,[1]† A. CHAVERNAS,[2] V. BARRÓN[2] AND J. TORRENT[2]

[1]Agronomy Department, Purdue University, West Lafayette, Indiana 47907, USA
[2]Departamento de Ciencias y Recursos Agrícolas y Forestales, Universidad de Córdoba, Apdo. 3048, 14080 Córdoba, Spain

Abstract—We measured the visible to near-infrared (IR) spectra of 176 synthetic and natural samples of Fe oxides, oxyhydroxides and an oxyhydroxysulfate (here collectively called "Fe oxides"), and of 56 soil samples ranging widely in goethite/hematite and goethite/lepidocrocite ratios. The positions of the second-derivative minima, corresponding to crystal-field bands, varied substantially within each group of the Fe oxide minerals. Because of overlapping band positions, goethite, maghemite and schwertmannite could not be discriminated. Using the positions of the $^4T_1 \leftarrow {}^6A_1$, $^4T_2 \leftarrow {}^6A_1$, $(^4E;{}^4A_1) \leftarrow {}^6A_1$ and the electron pair transition $(^4T_i + {}^4T_1) \leftarrow ({}^6A_1 + {}^6A_1)$, at least 80% of the pure akaganeite, feroxyhite, ferrihydrite, hematite and lepidocrocite samples could be correctly classified by discriminant functions. In soils containing mixtures of Fe oxides, however, only hematite and magnetite could be unequivocally discriminated from other Fe oxides. The characteristic features of hematite are the lower wavelengths of the $^4T_1$ transition (848–906 nm) and the higher wavelengths of the electron pair transition (521–565 nm) as compared to the other Fe oxides (909–1022 nm and 479–499 nm, resp.). Magnetite could be identified by a unique band at 1500 nm due to Fe(II) to Fe(III) intervalence charge transfer. As the bands of goethite and hematite are well separated, the goethite/hematite ratio of soils not containing other Fe oxides could be reasonably predicted from the amplitude of the second-derivative bands. The detection limit of these 2 minerals in soils was below 5 g kg^{-1}, which is about 1 order of magnitude lower than the detection limit for routine X-ray diffraction (XRD) analysis. This low detection limit, and the little time and effort involved in the measurements, make second-derivative diffuse reflectance spectroscopy a practical means of routinely determining goethite and hematite contents in soils. The identification of other accessory Fe oxide minerals in soils is, however, very restricted.

Key Words—Crystal Field Bands, Diffuse Reflectance Spectroscopy, Goethite, Hematite, Intervalence Charge Transfer, Iron Oxides, Magnetite.

INTRODUCTION

Diffuse reflectance spectroscopy in the visible (400–700 nm) and extended visible range (400–1200 nm) has been used as an ancillary method to identify and semiquantitatively estimate Fe oxides in clays, soils and sediments (Cornell and Schwertmann 1996, and references therein). Although spectra of samples with unknown mineralogy may simply be compared with spectra of reference minerals (Singer 1982; Morris et al. 1989), the parametrization of these spectra allows for a quantitative approach (Torrent and Barrón 1993). The most frequently used procedures for the parametrization are:

1) Calculation of the tristimulus values (*X, Y, Z*) of the CIE color system (CIE 1978). The tristimulus values are computed from the spectral reflectance and energy of the light source for each wavelength, and can be converted, by means of appropriate formulas or graphs, to the parameters of other color systems, such as Munsell or *L*a*b** (Wyszecki and Stiles 1982). Several indices based on such parameters have been correlated, for instance, with the hematite content, providing a semiquantitative estimation of this mineral in soils (Torrent et al. 1980; Barrón and Torrent 1986; Nagano et al. 1992, 1994).

2) Application of the Kubelka-Munk theory. With this method, the reflectance values, *R*, are used to obtain the remission function $F(R) = (1 - R)^2/(2R)$, which allows, in turn, calculation of the coefficients of absorption (*K*) and scattering (*S*) corresponding to the 2 phenomena involved in the sample-light interaction process. It has been shown that *K* and *S* are additive in a mixture of pigments. Therefore, one can estimate the concentration of an Fe oxide in the mixture by knowing the color characteristics of each of the components of the mixture, and assuming a standard color for the Fe oxides investigated (Barrón and Torrent 1986; Fernández and Schulze 1992).

3) Calculation of derivatives of the reflectance or the remission function to derive the position and intensity of the absorption bands. These bands are produced by crystal-field transitions of Fe(III) in an oc-

† Present address: Department of Plant and Soil Science, University of Delaware, Newark, Delaware 19717-1303 USA.

Table 1. References, origin (syn = synthetic, nat = natural), number (*N*) and Al substitution (Al-subst.) of the Fe oxide samples.

Fe oxide (abbreviation)	Origin (*N*)	Al-subst. (mole-fraction)	References
Akaganeite (Akag)	syn (7)	0	Bigham et al. (1990, 1996); Schwertmann et al. (1995)
Feroxyhyte (Feroxy)	syn (5)	0	Carlson and Schwertmann (1980)
Ferrihydrite (Ferrih)	syn (11) nat (11)	0	Schwertmann and Fischer (1973); Schwertmann et al. (1982); Schwertmann and Kämpf (1983); Carlson and Schwertmann (1981, 1987)
Goethite (Goeth)	syn (25) nat (36)	0–0.32	Schulze and Schwertmann (1984); Schwertmann et al. (1985)
Hematite (Hem)	syn (26) nat (20)	0–0.16	Stanjek (1991); Stanjek and Schwertmann (1992); Murad and Schwertmann (1986); Torrent and Schwertmann (1987)
Lepidocrocite (Lepido)	syn (14) nat (3)	0–0.14	Schwertmann and Fitzpatrick (1977); Carlson and Schwertmann (1990); Schwertmann and Wolska (1990); Murad and Schwertmann (1984)
Maghemite (Magh)	nat (3)	0–0.7	Taylor and Schwertmann (1974)
Magnetite (Magn)	syn (5)	0–0.17	Schwertmann and Murad (1990)
Schwertmannite (Schwt)	syn (4) nat (6)	0	Bigham et al. (1990, 1996); Schwertmann et al. (1995)

tahedral ligand field (Sherman and Waite 1985). Due to the combination of several polarization planes and particle-dependent scattering, the diffuse reflectance spectra of powders show broad, strongly overlapping bands (Kortüm 1969; Morris et al. 1982). To determine the positions of these bands, the resolution may be mathematically enhanced by calculating the derivatives of the measured spectra (Huguenin and Jones 1986). Deaton and Balsan (1991) used the first derivative, and Kosmas et al. (1984, 1986) and Malengreau et al. (1994, 1996) used the second derivative to detect and quantify different Fe oxides in soils or mineral mixtures. In a similar approach, Coyne et al. (1990) found that second-derivative spectra were superior to first derivative or untransformed spectra in predicting the amount of structural or interlayer Fe(III) in montmorillonite.

Recent studies have suggested very low detection limits for Fe oxides and the possibility of unequivocally differentiating between the various Fe oxides based on crystal field band positions (Malengreau et al. 1994, 1996). Since these studies were carried out for relatively simple mineral mixtures and with a limited number of Fe oxide samples, a closer examination of the potential of second-derivative reflectance spectroscopy seemed necessary. Thus, the objective of this work was to examine the ability of the second-derivative spectra to: 1) discriminate among different Fe oxides, and 2) help semiquantitatively estimate Fe oxide contents in soils, using a substantially larger collection of samples than those used in previous studies. We restricted this study to the evaluation of crystal field bands. The OH and H_2O vibrational bands in the IR constitute, however, another possibility for characterizing Fe oxides (Bishop et al. 1995; Bishop and Murad 1996).

MATERIALS AND METHODS

Synthetic and Natural Fe Oxides, and Soils

The origins of the Fe oxide samples are given in Table 1. The samples from natural environments include precipitates in spring waters, lake ores, concretions, NaOH-enriched soil fractions and whole soils. Forty soil samples with variable hematite-to-goethite ratios come from A or B horizons of soils from several countries of the European Union and Brazil, including Vertisols, Luvisols, Nitosols, Acrisols and Ferralsols. Determination of citrate/bicarbonate/dithionite-extractable iron (Fe_d) (Mehra and Jackson 1960), and acid oxalate-extractable iron (Fe_o) (Schwertmann 1964) and differential XRD (Schulze 1981) were carried out to estimate their hematite and goethite contents, which ranged between 0 and 150 g kg^{-1}. Sixteen samples with different lepidocrocite-to-goethite ratios are from crusts, pipestems and other Fe-oxide-enriched soil matrices from South Africa (Schwertmann and Fitzpatrick 1977).

Spectral Measurements

Diffuse reflectance spectra were obtained from dry and ground powders. For the hematitic soils, spectra were taken from 380 to 750 nm at 1-nm increments, using a Perkin-Elmer Lambda 3 spectrophotometer fitted with a reflectance attachment (Perkin Elmer, Norwalk, Connecticut, USA). $BaSO_4$ was used as a white standard. All other samples were measured between 200 and 2500 nm at 1-nm increments with a 20-cm integrating sphere (Labsphere, Inc., USA) attached to a Perkin-Elmer Lambda 19 (Überlingen, Germany). A Spectralon standard (Labsphere, Inc., USA) was used as reflectance reference. The wavelength-dependent reflectance functions were transformed into remission

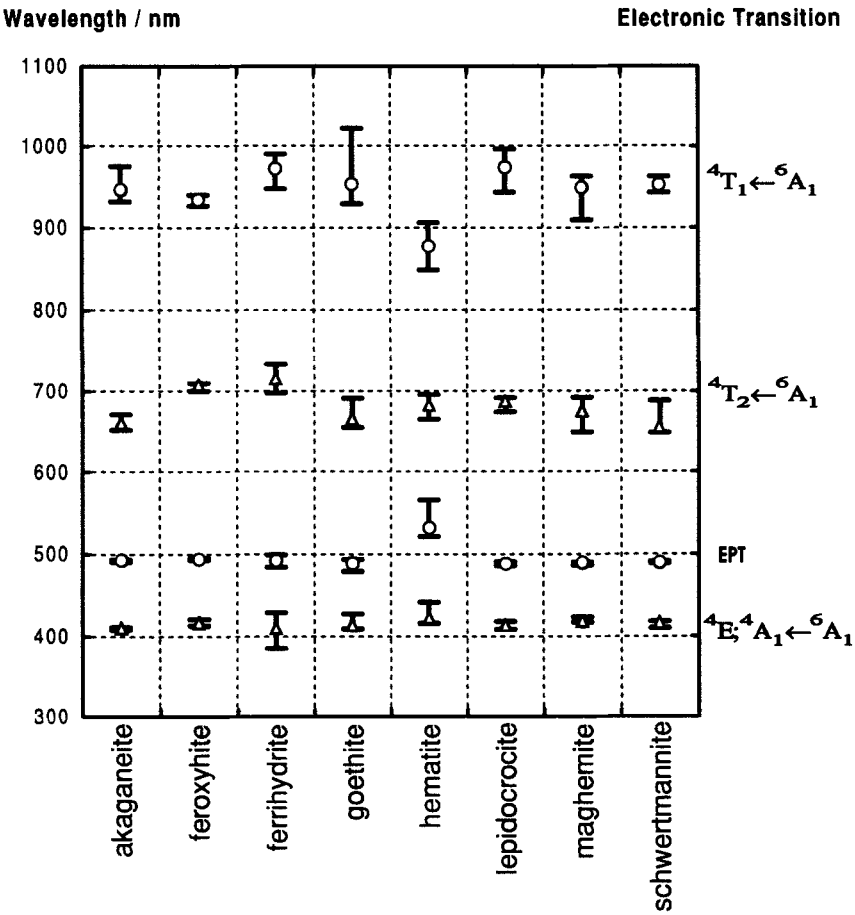

Figure 1. Median and range of the crystal field band positions determined by second-derivative minima.

functions. The first and the second derivatives were calculated using a cubic spline fitting procedure (Press et al. 1992). Briefly, a cubic spline consists of a number of cubic polynomial segments joined end to end with continuity in first and second derivatives in the joints. A crucial input parameter in the program is the number of points taken for each segment, which determines the goodness of fitting (r^2) and the degree of smoothing of the curve. Several tests showed 15 to be the optimum number of points to obtain smooth curves with high r^2 values; therefore, this number was adopted for the systematic calculation of the second-derivative curves. The selected smoothing parameters are not valid in general, but must be adjusted when the spectra are taken with different scan parameters.

RESULTS AND DISCUSSION

Discrimination between Single-Phase Fe Oxides

The second-derivative spectra revealed 4 bands in the range from 350 to 1050 nm. These bands were assigned, according to Sherman and Waite (1985), to the 3 single-electron transitions $^4T_1 \leftarrow {}^6A_1$, $^4T_2 \leftarrow {}^6A_1$ and $(^4E;{}^4A_1) \leftarrow {}^6A_1$, and the electron pair transition $(^4T_1 + {}^4T_1) \leftarrow (^6A_1 + {}^6A_1)$, in the following abbreviated by "EPT" (Figure 1).

The EPT, as the most intense absorption band, determines the position of the absorption edge which, in turn, is closely related to the hue. The EPTs for the hematites occur at 521 to 565 nm, clearly separated from the EPTs of the other, more yellowish Fe oxides (479 to 499 nm) (Table 2). The difference in EPT and color between hematite and the other Fe oxides has been explained by the presence of face-sharing octahedra in the hematite structure leading to an increase of the magnetic coupling between neighboring Fe(III) centers (Sherman and Waite 1985). In contrast to the results of Malengreau et al. (1994), however, the ranges of the EPT of all other Fe oxides generally overlapped, that is, the discrimination of these Fe oxides could not be performed with the EPT only.

A similar separation of hematite from the other Fe oxides is given by the $^4T_1 \leftarrow {}^6A_1$ transition (Figure 1).

https://doi.org/10.1346/CCMN.1998.0460506 Published online by Cambridge University Press

Table 2. Median and range of crystal field band positions (nm).

	$^4T_1$	$^4T_2$	EPT	(^4E; $^4A_1$)
Akaganeite	946	659	492	410
(N = 7)	932–975	652–671	490–493	408–411
Feroxyhyte	933	707	493	417
(N = 5)	926–940	700–710	492–495	413–421
Ferrihydrite	972	716†	492	410†
(N = 22)	947–990	698–734	484–499	386–410
Goethite	953	665	488	413
(N = 61)	929–1022	654–691	479–493	409–427
Hematite	877	682	531	423†
(N = 46)	848–906	664–695	521–565	416–442
Lepidocrocite	973	687	488	413
(N = 17)	943–997	673–692	485–490	408–418
Maghemite	948	675	489	418
(N = 3)	909–963	648–675	486–490	417–423
Schwertmannite	952	655	489	416†
(N = 10)	942–962	648–688	488–491	410–416

† Band not always determinable (no minimum of the second-derivative spectrum).

The significantly lower wavelength of this transition for hematite (848–906 nm) is the result of the lower crystal field splitting energy of hematite (14,000 cm^{-1}) as compared to that of goethite (15,320 cm^{-1}), maghemite (15,410 cm^{-1}) and lepidocrocite (15,950 cm^{-1}) (Burns 1993). Again, strongly overlapping band positions prevent a proper discrimination of the non-hematite Fe oxides by only this band.

With the $^4T_2 \leftarrow {}^6A_1$ transition at 698 to 734 nm, the ferrihydrite and feroxyhite samples are distinct from the other Fe oxides, where this transition occurs at lower wavelengths (648 to 695 nm) (Figure 1, Table 2). Sixteen out of 22 ferrihydrite samples did not show, however, a second-derivative minimum, so that the band position could not be determined. The $(^4E;^4A_1) \leftarrow {}^6A_1$ transition of all Fe oxides ranged from 386 to 442 nm. This band was not visible in the derivative spectra of 25 hematites.

To evaluate the discriminative power of the positions of all 4 bands combined, a stepwise discriminant analysis was performed (StatSoft Inc. 1996). The *a priori* probabilities were assumed to be equal for all Fe oxide minerals, in order to avoid the predominant classification of minerals with the larger numbers of samples which, in turn, would decrease the sensitivity of classification for the small mineral groups. To allow for the inclusion of all samples, we split the groups of both ferrihydrite and hematite into subgroups containing all 4 bands, and into subgroups where 1 band was missing and set to zero. Table 3 shows that all feroxyhite, ferrihydrite and hematite samples were correctly classified by using the 4 bands, and more than 80% of the akaganeite and lepidocrocite samples were correctly discriminated. The band positions of goethite, maghemite and schwertmannite are, however, too similar to allow for a reliable discrimination (Table 3).

Table 3. Classification of Fe oxides by $^4T_1$, $^4T_2$, EPT and (^4E; $^4A_1$). Rows: observed classifications; columns: predicted classifications.

	Percent correct	Akag	Feroxy	Ferrih $-{}^4T_2$	Ferrih $+{}^4T_2$	Goeth	Hem + (E;A)	Hem − (E;A)	Lepido	Magh	Schwt
Akaganeite	83	5	0	0	0	0	0	0	0	1	0
Feroxyhite	100	0	5	0	0	0	0	0	0	0	0
Ferrihdyrite $-{}^4T_2$†	100	0	0	16	0	0	0	0	0	0	0
Ferrihdyrite $+{}^4T_2$†	100	0	0	0	6	0	0	0	0	0	0
Goethite	23	8	0	0	0	14	0	0	3	13	22
Hematite $+(^4E;^4A_1)$†	100	0	0	0	0	0	21	0	0	0	0
Hematite $-(^4E;^4A_1)$†	100	0	0	0	0	0	0	22	0	0	0
Lepidocrocite	81	0	0	0	0	0	0	0	13	3	0
Maghemite	33	0	0	0	0	0	0	0	1	1	1
Schwertmannite	50	1	0	0	0	2	0	0	1	0	4
Total	66	14	5	16	6	16	21	22	18	18	27

† Ferrihydrite $-{}^4T_2$: ferrihydrite samples without the $^4T_2$ band, Ferrihydrite $+{}^4T_2$: ferrihydrite samples with the $^4T_2$ band. Hematites resp. with and without the (^4E;$^4A_1$) band.

https://doi.org/10.1346/CCMN.1998.0460506 Published online by Cambridge University Press

Table 4. Coefficients of the classification function (see text).

	Akag	Feroxy	Ferrih $+{}^4T_2$	Goeth	Hem +(E;A)	Lepid	Magh	Schwt
a_x	14.92	15.80	16.02	14.98	15.43	15.36	15.09	14.92
b_x	26.21	26.43	26.53	26.09	27.61	26.24	26.09	26.16
c_x	0.26	0.25	0.22	0.26	0.26	0.26	0.26	0.26
d_x	8.62	8.57	8.86	8.67	8.33	8.78	8.59	8.68
e_x	−15,504	−16,158	−16,640	−15,527	−16,295	−15,961	−15,529	−15,535

A set of classification functions to determine the Fe oxide mineralogy of further samples is given by:

$$S_x = a_x \cdot {}^4T_2 + b_x \cdot \mathrm{EPT} + c_x \cdot ({}^4\mathrm{E};\, {}^4\mathrm{A}_1) + d_x \cdot {}^4T_1 + e_x \quad [1]$$

with the scores for each group of minerals, S_x, and the coefficients for each group, a_x, b_x, c_x, d_x and e_x as defined in Table 4. Within the limitations shown before, the highest number of S_x gives the Fe oxide mineral of the examined sample. As second-derivative spectra without a minimum in the ${}^4\mathrm{T}_2 \leftarrow {}^6\mathrm{A}_1$ range unequivocally indicated ferrihydrite, and those without a minimum in the $({}^4\mathrm{E};{}^4\mathrm{A}_1) \leftarrow {}^6\mathrm{A}_1$ range unequivocally indicated hematite, no classification functions are necessary for these subgroups. As the band positions derived from the second derivatives depend on the x and y units of the spectra, and on the smoothing of the spectra, it is indispensable to follow the procedure given under Materials and Methods before calculating the scores.

Identification of Mixtures of Fe Oxides

Because of the well-separated EPTs of goethite and hematite, both phases are clearly detectable from the derivative spectra of soils (Figure 2). The intensity of the minima depends on the goethite-to-hematite ratio (see below).

Although lepidocrocite and goethite could be discriminated in pure phases (Table 2), the derivative spectra of soils containing both Fe oxides did not resolve the slightly different band positions (Figure 3). Using the classification functions given in Table 4, soils with lepidocrocite/(lepidocrocite + goethite) ≥0.37 were classified as lepidocrocites, while those with a ratio ≤0.37 were classified as goethite or maghemite. In the same way, the derivative spectra of ferrihydrite/goethite and ferrihydrite/lepidocrocite mixtures did not resolve the bands of both phases (data not shown). That is, second-derivative spectroscopy is not suited to detect small amounts of ferrihydrite or lepidocrocite in addition to a major goethite phase—a situation which should frequently occur in soils due to thermodynamic inequilibria (Cornell and Schwertmann 1996). Although not tested experimentally, it may be concluded that spectra of other combinations of Fe oxides with band positions in the same or strongly overlapping regions would not allow the single contributions to be resolved, either.

Besides the band wavelengths, absolute and relative band intensities and bandwidths may be used to dis-

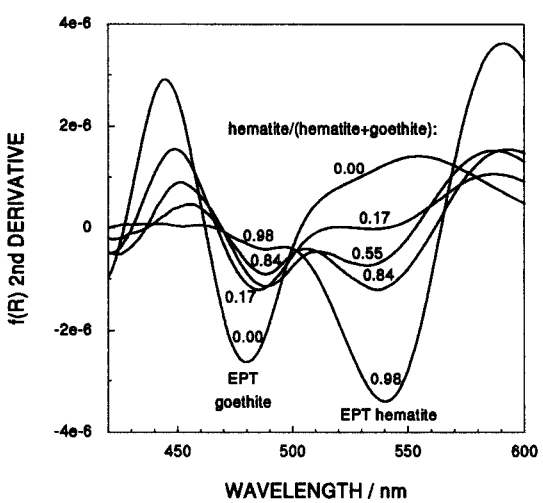

Figure 2. Second-derivative spectra of soils with various hematite/(hematite + goethite) ratios.

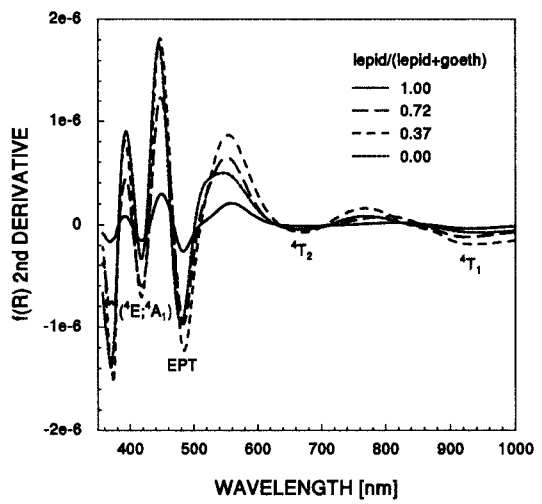

Figure 3. Second-derivative spectra of soils with various lepidocrocite/(lepidocrocite + goethite) ratios.

https://doi.org/10.1346/CCMN.1998.0460506 Published online by Cambridge University Press

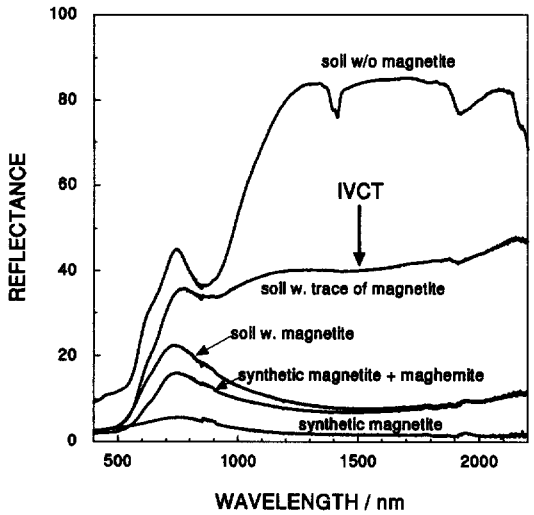

Figure 4. Reflectance spectra of pure magnetite, magnetite + maghemite and soils with various concentrations of magnetite.

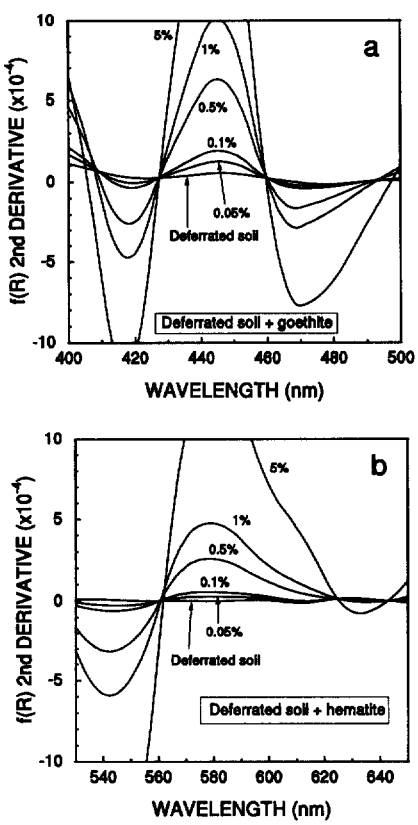

Figure 5. Second-derivative spectra of the remission function $f(R)$ in selected spectrum bands for mixtures of a deferrated soil material with different quantities of (a) goethite and (b) hematite.

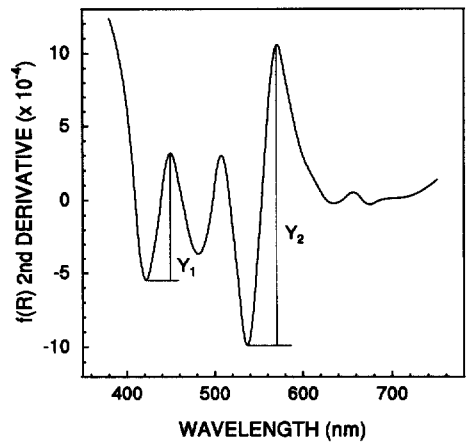

Figure 6. Position and amplitude of the bands selected for the quantification of goethite (Y_1) and hematite (Y_2) in soil samples.

criminate Fe oxides. Although such differences were evident with synthetic, single-phase samples, for example, sharper bands for goethite than for ferrihydrite, these differences were generally less expressed for natural Fe oxides, and could not be used to differentiate the origin of overlapping bands in mixtures and soils. Band amplitudes of the second-derivative spectra were higher for hematite, but no significant differences were found between the amplitudes of the other Fe oxides.

The reflectance of the magnetite samples was very low and, because of that, the spectra were too noisy to allow for the determination of their crystal field bands. This low reflectivity is caused by a strong absorption band which has its maximum in the near-IR at about 1500 nm, but extends across the visible range (Figure 4). It is caused by the presence of Fe(II) and Fe(III) in neighboring octahedra in the magnetite structure, leading to the delocalization of electrons due to intervalence charge transfer (IVCT) (Sherman and Waite 1985; Burns 1981). Strens and Wood (1979) determined the position of the IVTC of magnetite from diffuse reflectance spectra at 1400 nm, and Sherman (1987) derived an energy of 1475 nm from molecular orbital calculations assuming equal sites for Fe(II) and Fe(III) ($q = 0$). Both values correspond with ours, considering the low precision with which the position of such broad bands could be determined. The shape of this IVCT band is more pronounced in samples of maghemite–magnetite mixtures, or in soils containing magnetite, because of the generally higher reflectivity of these samples (Figure 4). Even trace amounts of magnetite are detectable.

Quantification of Hematite and Goethite in Soils

The well-separated EPTs of goethite and hematite allow one to identify very small amounts of goethite and hematite. Figure 5 shows selected parts of the sec-

https://doi.org/10.1346/CCMN.1998.0460506 Published online by Cambridge University Press

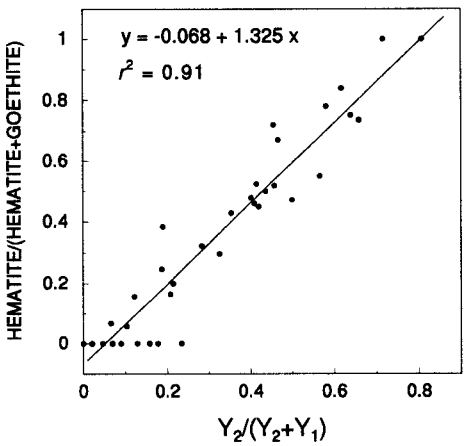

Figure 7. The relationship between the hematite/(hematite + goethite) ratio as determined by differential XRD, and the $Y_2/(Y_1 + Y_2)$ ratio as determined by diffuse reflectance spectroscopy (see Figure 6 for explanation of Y_1 and Y_2).

ond-derivative curve of the reflectivity function for mixtures of a deferrated soil matrix (treated with citrate/bicarbonate/dithionite to remove Fe oxides) and synthetic hematite and goethite; concentrations as low as 0.5 g kg^{-1} produce a significant change in the curve. In Vertisol samples containing only goethite as Fe oxide, the detection limit for this mineral was about 3 g kg^{-1} (results not shown). In summary, the detection limit seems to be at least 1 order of magnitude smaller than that of ordinary XRD.

To obtain an index of the band intensity in the second-derivative curves for goethite and hematite, we used the amplitude between the ~415-nm minimum ($(^4E;^4A_1)\leftarrow{}^6A_1$) and the ~445-nm maximum for goethite (denoted as Y_1), and between the ~535-nm minimum (EPT) and the ~580-nm maximum for hematite (denoted as Y_2) (Figure 6). For the 40 soils used, which generally contained less than 150 g kg^{-1} hematite and goethite, a highly significant correlation was found between goethite content and Y_1 (Goethite [g kg^{-1}] = $-0.06 + 268Y_1$; $r^2 = 0.86$; $P < 0.001$), and hematite content and Y_2 (Hematite [g kg^{-1}] = $-0.09 + 402Y_2$; $r^2 = 0.85$; $P < 0.001$). Multiple regression using both amplitudes did not improve the correlation coefficient. For the same soils, the redness rating, (R_{CIE}), proposed by Barrón and Torrent (1986) provided a higher correlation with the hematite content ($r^2 = 0.94$). However, the procedures based on the second-derivative curve have the advantage over redness ratings in that they help simultaneously predict hematite and goethite contents. In practice, one can use the relationship between the hematite/(hematite + goethite) ratio (derived from X-ray or differential XRD measurements) and the $Y_2/(Y_1 + Y_2)$ amplitude ratio for that purpose (Figure 7). The absolute quantities of hematite and goethite are calculated from the predicted hematite/(hematite + goethite) ratio, by assigning the difference between citrate/bicarbonate/dithionite-extractable Fe and oxalate-extractable Fe to hematite and goethite.

CONCLUSIONS

Modern spectrophotometers allow the fast acquisition of reflectance spectra (typically less than 10 min, only a few seconds with new diode array detectors), and calculations of derivatives and band amplitudes can be done easily with the appropriate software. In addition, sample preparation for spectrophotometric measurements is fast (<5 min) and nondestructive. These advantages make second-derivative diffuse reflectance spectroscopy well suited for routine measurements of goethite and hematite in soils and mineral mixtures. With the exception of hematite and magnetite, however, the unequivocal discrimination of Fe oxide minerals cannot be performed by using the positions of the crystal field bands only. A better result may be achieved by including the vibrational bands into the discriminant analysis (Coyne et al. 1990; Bishop et al. 1995; Bishop and Murad 1996).

ACKNOWLEDGMENTS

ACS acknowledges the research grant by the Deutsche Forschungsgemeinschaft, and thanks D. G. Schulze (Purdue University) who gave the visiting scientist a warm welcome and provided the equipment, R. V. Morris (NASA, Houston, Texas) for his introduction into the secrets of diffuse reflectance spectroscopy and U. Schwertmann (Technische Universität München, Germany) who generously provided his large collection of Fe oxides.

REFERENCES

Barrón V, Torrent J. 1986. Use of the Kubelka-Munk theory to study the influence of iron oxides on soil colour. J Soil Sci 37:499–510.

Bigham JM, Schwertmann U, Carlson L, Murad E. 1990. A poorly crystallized oxyhydroxysulfate of iron formed by bacterial oxidation of Fe(II) in acid mine waters. Geochim Cosmochim Acta 54:2743–2758.

Bigham JM, Schwertmann U, Pfab G. 1996. Influence of pH on mineral speciation in a bioreactor simulating acid mine drainage. Appl Geochem 11:845–852.

Bishop JL, Murad E. 1996. Schwertmannite on Mars? Spectroscopic analyses of schwertmannite, its relationship to other ferric minerals, and its possible presence in the surface material on Mars. In: Dyar MD, McCammon C, Schaefer MW, editors. Mineral spectroscopy: A tribute to Roger G. Burns. Spec Publ: Geochem Soc.

Bishop JL, Pieters CM, Burns RG, Edwards JO, Mancinelli RL, Froeschl H. 1995. Reflectance spectroscopy of ferric sulfate-bearing montmorillonites as Mars soil analog materials. Icarus 117:101–119.

Burns RG. 1981. Intervalence transitions in mixed-valence minerals of iron and titanium. Ann Rev Earth Planet Sci 9: 345–383.

Burns RG. 1993. Mineralogical applications of crystal field theory. Cambridge topics in mineral physics and chemistry, 5. Cambridge Univ Pr. 551 p.

Carlson L, Schwertmann U. 1980. Natural occurrence of feroxyhite (δ-FeOOH). Clays Clay Miner 28:272–280.

Carlson L, Schwertmann U. 1981. Natural ferrihydrites in surface deposits from Finland and their association with silica. Geochim Cosmochim Acta 45:421–429.

Carlson L, Schwertmann U. 1987. Iron and manganese oxides in Finnish ground water treatment plants. Wat Res 21:165–170.

Carlson L, Schwertmann U. 1990. The effect of CO_2 and oxidation rate on the formation of goethite versus lepidocrocite from an Fe(II) system at pH 6 and 7. Clay Miner 25:65–71.

CIE. 1978. Recommendations on uniform color spaces, color difference and psychometric color terms. Colorimetry, Suppl. 2 to Publ 15. Paris: CIE.

Cornell RM, Schwertmann U. 1996. The iron oxides: Structure, properties, reactions, occurrence and uses. Weinheim: VCH Verlagsgesellschaft. 573 p.

Coyne LM, Bishop JL, Scattergood T, Banin A, Carle G, Orenberg J. 1990. Near-infrared correlation spectroscopy: Quantifying iron and surface water in a series of variably cation-exchanged montmorillonite clays. In: Coyne LM, McKeever WS, Blake DF, editors. Spectroscopic characterization of minerals and their surfaces. Am Chem Soc. p 407–429.

Deaton BC, Balsam WL. 1991. Visible spectroscopy. A rapid method for determining hematite and goethite concentration in geological materials. J Sediment Petrol 61:628–632.

Fernández RN, Schulze DG. 1992. Munsell colors of soils simulated by mixtures of goethite and hematite with kaolinite. Z Pflanzenernähr Bodenk 155:473–478.

Huguenin RL, Jones JL. 1986. Intelligent information extraction from reflectance spectra: Absorption band positions. J Geophys Res 91:9585–9598.

Kortüm G. 1969. Reflectance spectroscopy. New York: Springer-Verlag. 366 p.

Kosmas CS, Curi N, Bryant RB, Franzmeier DP. 1984. Characterization of iron oxide minerals by second-derivative visible spectroscopy. Soil Sci Soc Am J 48:401–405.

Kosmas CS, Franzmeier DP, Schulze DG. 1986. Relationship among derivative spectroscopy, color, crystallite dimensions, and Al substitution of synthetic goethites and hematites. Clays Clay Miner 34:625–634.

Malengreau N, Bedidi A, Muller J-P, Herbillon AJ. 1996. Spectroscopic control of iron oxide dissolution in two ferralitic soils. Eur J Soil Sci 47:13–20.

Malengreau N, Muller J-P, Calas G. 1994. Fe-speciation in kaolins: A diffuse reflectance study. Clays Clay Miner 42: 137–147.

Mehra OP, Jackson ML. 1960. Iron oxide removal from soils and clays by a dithionite-citrate system buffered with sodium bicarbonate. Clays Clay Miner 7:317–327.

Morris RV, Agresti DG, Lauer HV, Newcomb JA, Shelfer TD, Murali AV. 1989. Evidence for pigmentary hematite on Mars based on optical, magnetic, and Mössbauer studies of superparamagnetic (nanocrystalline) hematite. J Geophys Res 94:2760–2778.

Morris RV, Neely SC, Mendell WW. 1982. Application of Kubelka-Munk theory of diffuse reflectance to geologic problems: The role of scattering. Geophys Res Lett 9:113–116.

Murad E, Schwertmann U. 1984. The influence of crystallinity on the Mössbauer spectrum of lepidocrocite. Mineral Mag 48:507–511.

Murad E, Schwertmann U. 1986. Influence of Al substitution and crystal size on the room-temperature Mössbauer spectrum of hematite. Clays Clay Miner 34:1–6.

Nagano T, Nakashima S, Nakayama S, Osada K, Senoo M. 1992. Color variations associated with rapid formation of goethite from proto-ferrihydrite at pH 13 and 40° C. Clays Clay Miner 40:600–607.

Nagano T, Nakashima S, Nakayama S, Senoo M. 1994. The use of color to quantify the effects of pH and temperature on the crystallization kinetics of goethite under highly alkaline conditions. Clays Clay Miner 42:226–234.

Press WH, Teukolsky SA, Vetterling WT, Flannery BP. 1992. Numerical recipes in Fortran. The art of scientific computing. Cambridge Univ Pr. 963 p.

Schulze DG. 1981. Identification of soil iron oxide minerals by differential X-ray diffraction. Soil Sci Soc Am J 45: 437–440.

Schulze DG, Schwertmann U. 1984. The influence of aluminium on iron oxides: X. Properties of Al-substituted goethites. Clay Miner 19:521–529.

Schwertmann U. 1964. Differenzierung der Eisenoxide des Bodens durch Extraktion mit Ammoniumoxalat-Lösung. Zeitschrift für Pflanzenernähr Dögung and Bodenkunde 105:194–202.

Schwertmann U, Bigham JM, Murad E. 1995. The first occurence of Schwertmannite in a natural stream environment. Eur J Mineral 7:547–552.

Schwertmann U, Cambier P, Murad E. 1985. Properties of goethites of varying crystallinity. Clays Clay Miner 33: 369–378.

Schwertmann U, Fischer WR. 1973. Natural "amorphous" ferric hydroxide. Geoderma 10:237–247.

Schwertmann U, Fitzpatrick RW. 1977. Occurrence of lepidocrocite and its association with goethite in Natal soils. Soil Sci Soc Am J 41:1013–1018.

Schwertmann U, Kämpf N. 1983. Óxidos de ferro jovens em ambientes pedogenéticos brasileiros. R bras Ci Solo 7:251–255.

Schwertmann U, Murad E. 1990. The influence of aluminum on iron oxides: XIV. Al-substituted magnetite synthesized at ambient temperatures. Clays Clay Miner 38:196–202.

Schwertmann U, Schulze DG, Murad E. 1982. Identification of ferrihydrite in soils by dissolution kinetics, differential X-ray diffraction, and Moessbauer spectroscopy. Soil Science Soc Am J 46:869–875.

Schwertmann U, Wolska E. 1990. The influence of aluminum on iron oxides: XV. Al-for-Fe substitution in synthetic lepidocrocite. Clays Clay Miner 38:209–212.

Sherman DM. 1987. Molecular orbital (SCF-Xa-SW) theory of metal-metal charge transfer processes in minerals: I. Application to $Fe^{2+} \rightarrow Fe^{3+}$ charge transfer and "electron delocalization" in mixed-valence iron oxides and silicates. Phys Chem Miner 14:355–363.

Sherman DM, Waite TD. 1985. Electronic spectra of Fe^{3+} oxides and oxide hydroxides in the near IR to near UV. Am Mineral 70:1262–1269.

Singer RB. 1982. Spectral evidence for the mineralogy of high-albedo soils and dust on Mars. J Geophys Res 87: 10159–10168.

Stanjek H. 1991. Aluminium- und Hydroxylsubstitution in synthetischen und natürlichen Hämatiten [PhD thesis]. Technische Universität München, Freising. 194 p.

Stanjek H, Schwertmann U. 1992. The influence of aluminum on iron oxides. Part XVI: Hydroxyl and aluminum substitution in synthetic hematites. Clays Clay Miner 40:347–354.

StatSoft Inc. 1996. Statistica for Windows. Tulsa, OK.

Strens RGJ, Wood BJ. 1979. Diffuse reflectance spectra and optical properties of some iron and titanium oxides and oxyhydroxides. Mineral Mag 43:347–354.

Taylor RM, Schwertmann U. 1974. Maghemite in soils and its origin. I. Properties and observations on soil maghemites. Clay Miner 10:289–298.

Torrent J, Barrón V. 1993. Laboratory measurements of soil color: Theory and practice. In: Bigham JM, Ciolkosz EI, editors. Soil color. SSSA Spec Publ. Madison, WI: Soil Sci Soc Am. p 21–33.

Torrent J, Schwertmann U. 1987. Influence of hematite on the color of red beds. J Sediment Petrol 57:682–686.

Torrent J, Schwertmann U, Schulze DG. 1980. Iron oxide mineralogy of some soils of two river terrace sequences in Spain. Geoderma 23:191–208.

Wyszecki G, Stiles WS. 1982. Color science: Concepts and methods, quantitative data and formulae. New York: J. Wiley. 950 p.

(Received 28 August 1997; accepted 23 January 1998; Ms. 97-084)